Available online at www.sciencedirect.com

ScienceDirect

Energy Procedia 66 (2015) 37 – 40

Energy Procedia

The 12th International Conference on Combustion & Energy Utilisation – 12ICCEU

Effect of diesel engine operating conditions on the particulate size, nanostructure and oxidation properties when using wasting cooking oil biodiesel

X.J. Man[1]*, C.S. Cheung[1], Z. Ning[2]

[1]*Department of Mechanical Engineering, The Hong Kong Polytechnic University, Hung Hom, Kowloon, Hong Kong*
[2]*School of Energy and Environment, City University of Hong Kong, Tat Chee Avenue, Kowloon, Hong Kong*

Abstract

Present work focuses on the effect of engine operating parameters, including the engine speed and engine load (air/fuel ratio), on the particulate nanostructure and oxidative reactivity when the engine is operated with WCO (waste cooking oil) biodiesel. The particulate samples were collected from the diluted exhaust produced by a medium-duty direct injection diesel engine and were used to analyze the physical and chemical properties via using the high-resolution transmission electron microscope (TEM) and the thermogravimetric analysis/differential scanning calorimetry (TGA/DSC). The TEM images reveal that larger primary particles are formed at low engine speed and high engine load. The particles with typical inner core-outer shell structure are common at high engine load due to the sufficiently high in-cylinder gas temperature and pressure. Quantitative analysis of the nanostructures indicates stronger effect in engine load than engine speed and more soot with shorter and more curving graphene layer at lower engine load. Furthermore, the results of TGA infer that the soot oxidative reactivity is closely related to the nanostructure and the effect of engine load at constant engine speed is more pronounced than the effect of engine speed.

Peer-review under responsibility of the Engineering Department, Lancaster University

Keywords: diesel engine; biodiesel; primary particle; particulate oxidation

1. Introduction

Alternative fuels have been investigated and proposed for the partial or total replacement of diesel fuel to reduce reliance on fossil fuel and to reduce air pollution. Among these alternative fuels, biodiesel has received particular attention due to its renewability, potential of reducing greenhouse gas emissions, and inhibition of soot formation [1]. Furthermore, biodiesel can be directly fueled to a diesel engine without modification but NO_x emission would increase and the negative effect on human health and the environment still exist [2]. As a result, detailed investigations on the physical and chemical properties of the particulate matters (PM) emitted from an engine operating with biodiesel are required to provide fundamental knowledge to address the issues. A review of the literature shows that few works have been carried out on quantifying the nanostructure and oxidation properties of biodiesel soot [3-8]. This study focuses on investigating the influence of engine operating modes on the physico-chemical properties of

* Corresponding author. Tel.: +852 2766 7819; Fax: +852 2365 4703
E-mail address: xingjiaman@gmail.com

Peer-review under responsibility of the Engineering Department, Lancaster University
doi:10.1016/j.egypro.2015.02.020

the PM emitted by a diesel engine operating with waste cooking oil biodiesel. The PM properties investigated include primary particle size, nanostructure and oxidative reactivity.

2. Experimental approach

PM were sampled from the exhaust of a pre-Euro naturally aspirated, water-cooled, 4-cylinder 4.3-litre direct-injection diesel engine (ISUZU 4HF1). The biodiesel used was manufactured from waste cooking oil by Dynamic Progress Ltd., complying EN14214. The engine was operated under five operating modes, with detailed operating conditions listed in table 1. Modes 1, 2, 3 have similar high torque but different engine speeds (low, high and middle engine speed respectively); while modes 3, 4, 5 have the same middle engine speed but high, medium and low torques respectively. Thus effects of both engine loads and engine speeds can be investigated. Particulate samples for physico-chemical analysis were collected on 47 mm quartz fiber filter paper (ADVANTEC Corporation) and analysed with a high-resolution transmission electron microscope (HRTEM; Tecnai G2 20 S-TWIN Philips) and a thermogravimetric analyzer (Netzch STA 449 TGA/DSC) to investigate the primary particle size, nanostructure and oxidation reactivity. All the methods used in present work are described in [6].

3. Results and discussions

3.1 Size of primary particle

The TEM and HRTEM images reveal underlying structure of carbonaceous particulates and give an intuitive impression for the particulate size and morphology. Figure 1(a) suggests formations of clusters of fractal-structures, called agglomerates, with tens or hundreds of primary particles attached. Typical primary particle size distributions are shown in Fig. 1(b) for mode 1. Basically the primary particle size is normally distributed in each engine mode, with diameters varying from 10 to 50 nm. The mean diameters (D_p) of the primary particles and their standard deviations (sd) are listed in table 1 for each mode. It is observed that more primary particles with smaller diameter are formed at higher speed or lower engine load. The determined D_p decreases with the increase of engine speed or the decrease of engine load. These results from WCO biodiesel are in line with those from diesel reported by Lapuerta et al. [9].

Table 1. Engine test conditions, primary particle size, nanostructure parameters and oxidative characteristic

Test mode	speed (rpm)	Torque (Nm)	D_p(sd) (nm)	L_a (sd) (nm)	T_f (sd) (nm)	D_s (sd) (nm)	Volatiles (%)	T_i (^oC)	E (kJ/mol)	A (S^{-1})
1	1280	216	26.08 (2.50)	0.754 (0.0637)	1.226 (0.0521)	0.387 (0.011)	14.3±0.72	537.7	110.6±1.51	8.97×10^4
2	2560	216	23.87 (2.29)	0.747 (0.0409)	1.215 (0.0589)	0.382 (0.010)	17.8±0.98	533.6	114.2±1.54	1.84×10^5
3	1920	224	24.46 (1.97)	0.749 (0.0873)	1.237 (0.0705)	0.383 (0.011)	17.0±0.85	528.9	107.0±1.28	6.36×10^4
4	1920	112	21.30 (1.91)	0.731 (0.0213)	1.317 (0.0296)	0.375 (0.008)	47.9±2.54	508.5	90.6±1.78	8.12×10^3
5	1920	56	20.52 (2.13)	0.707 (0.0212)	1.391 (0.0413)	0.373 (0.015)	58.5±2.63	485.8	77.8±2.09	1.50×10^3

The size of primary particles is closely related to the combustion process. For modes 1-3, combustion process takes place at almost the same engine load and hence in-cylinder temperature. Higher engine speed leads to more unburned biodiesel due to shorter residence time inside the engine cylinder, making more chance for the formation of smaller nucleated particles. On the other hand, at lower engine speed, the extended diffusion combustion duration can promote particle nucleation and surface growth, leading to larger sized primary particles. For modes 3-5, the combustion proceeds in the same engine speed but under different engine loads. At lower engine load, there are lower in-cylinder temperature and pressure and shorter combustion duration, which slow down the generation and growth of the nuclei and

hence favour the formation of smaller primary particles. In contrary, the higher in-cylinder temperature and pressure, associated with the larger amount of fuel being burned and the longer combustion duration, leads to the formation of larger primary particles.

3.2 Nanostructure of primary particle

In order to further quantify the degree of nanostructure and type of soot, fringe length (L_a), tortuosity (T_f) and separation distance (D_s) were measured from the HRTEM images, as shown in Figure 1(c) and (d). The definitions of L_a, T_f, D_s are detailed in [6]. The median L_a, the mean T_f and the mean D_s for each mode, as well as their corresponding standard deviations, are listed in table 1. For modes 1-3, the nanostructure parameters reveal minor deviation with 95% confidence level, indicating limited impact of engine speed on the nanostructure. From the observation of TEM images, the typical inner core-outer shell structure, which contains longer and straighter graphene layers, is common at high engine load. Furthermore, as suggested by Hurt et al, [10], this core-shell nanostructure is the equilibrium configuration of nearly planar poly-aromatic clusters under the high-temperature reactive conditions of soot formation. Therefore, the primary particles for modes 1-3, formed in similar in-cylinder temperature and pressure, have similar stable graphitization nanostructure.

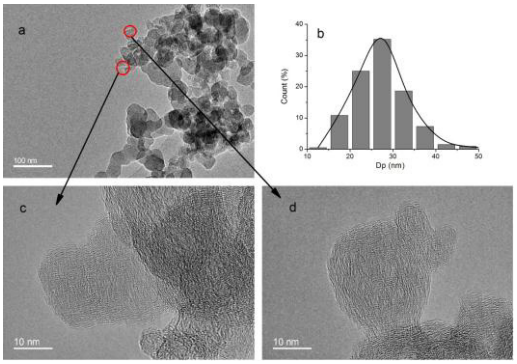

Figure 1. TEM and HRTEM images for mode 1.

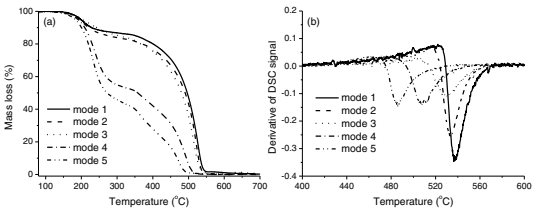

Figure 2. Mass loss curves and derivative of DSC signals of different particle samples for modes 1-5

The operating conditions of modes 3-5 are used to qualitatively analyse the influence of engine load on the nanostructure. From table 1, L_a decreases and T_f increases with the increase of the engine load, revealing that more particles exhibit an unordered configuration with shorter and more curving graphene layer at lower engine load. This is because that at lower engine load, the temperature and pressure can support the nucleation but not the growth to the equilibrium configuration.

3.3 Oxidation characteristics

A thermogravimetric analysis/differential scanning calorimetry (TGA/DSC) was used to oxidize WCO biodiesel particulate samples for modes 1-5. Figure 2 (a)-(b) show the mass loss curves and the derivative of DSC signals. Obviously, the mass loss curve for each mode shows two sharp decreases: one occurring at around 200-300^{o}C and the other occurring from 350-550^{o}C, which respectively is mainly caused by the loss of the volatile substances and the oxidation of the non-volatile substances. The temperature-history of derivative of DSC signals for each mode presents a sudden reduction at the temperature range of 450 to 550^{o}C, indicating a fast rate of mass loss and heat release. The temperature corresponding to the peak of this curve with the maximum rate of mass loss and heat release is defined as the ignition temperature (T_i). The volatiles fraction and T_i for modes 1-5 are listed in table 1, revealing that the influence of engine load (air/fuel ratio) is more pronounced than that of engine speed.

For further investigation on the oxidative property of the non-volatile substances, kinetic parameters are derived from the mass loss rate using a modified form of the Arrhenius expression, as suggested by

Stratakis and Stamatelos [11]. The kinetic parameters, including the pre-exponential factor (*A*) and activation energy (*E*), are determined and listed in table 1 for modes 1-5. The activation energy shows almost the same value of 110 *kJ/mol* and the pre-exponential factor is around 1.0×10^5 s^{-1} for modes 1-3, implying similar oxidative rate while *E* and *A* decrease as the engine load decreases for modes 3-5, indicating a faster oxidative rate at lower engine load.

The soot oxidative reactivity is closely related to the nanostructure including the size, orientation and organization of the graphene layers [3]. The degree of disorder of the carbonaceous nanostructure increases with the accessible carbons on the edge sites. Moreover, a carbon atom at an edge site is more reactive than one in the basal plane of a graphene layer because the surface oxygen functional groups bounded to edge sites can induce more micropore structures during attack by air on the edge sites[12]. Therefore, a soot particle with disordered configuration has more edge sites and hence has higher reactivity. As described in the section of nanostructure, the disordered structure with shorter and more curving fringe is prevailing under lower engine load, hence leading to lower ignition temperature.

4. Conclusions

This study focuses on the impact of engine operating parameters on the nanostructure and oxidative reactivity of WCO (waste cooking oil) biodiesel particulates. The TEM and HRTEM images reveal that the size and configuration of primary particles are determined by the combustion process. More particles with larger size and slightly aggregated structure can be found at lower engine speed while the primary particles tend to form the disordered amorphous structure at lower engine load. Moreover, the parameters of nanostructure measured from the HRTEM images are only slightly affected by the engine speed but significantly affected by the engine load. The shorter and more curving graphene layer was found in the particulate matters collected from lower engine load. Additionally, the soot oxidative reactivity is closely related to the nanostructure properties and volatiles. The impact of engine load at constant engine speed is more pronounced than the impact of engine speed.

Acknowledgment

The authors would like to acknowledge the financial support from The Hong Kong Polytechnic University (project no. B-Q33D) and the Research Grants Council of the Hong Kong SAR (project no. PolyU 5130/12E).

Reference

[1] R. Arvidsson, K. Fransson, M. Fröling, M. Svanström, S. Molander. (2012). *J Cleaner Prod*. **31**(0):54-61.
[2] G.L. Finch, C.H. Hobbs, L.F. Blair, E.B. Barr, F.F. Hahn, R.J. Jaramillo, J.E. Kubatko, T.H. March, R.K. White, J.R. Krone, M.G. Ménache, K.J. Nikula, J.L. Mauderly, J. Van Gerpen, M.D. Merceica, B. Zielinska, L. Stankowski, K. Burling, S. Howell. (2002). *Inhalation Toxicol*. **14**(10):1017-48.
[3] A.L. Boehman, J. Song, M. Alam. (2005). *Energy Fuels*. **19**(5):1857-64.
[4] H. Jung, D.B. Kittelson, M.R. Zachariah. (2006). *Int J Environ Sci Technol*. **40**(16):4949-55.
[5] M. Salamanca, F. Mondragón, J.R. Agudelo, A. Santamaría. (2012). *Atmos Environ*. **62**(0):220-7.
[6] T. Lu, C.S. Cheung, Z. Huang. (2012). *J Aerosol Sci*. **47**(0):27-38.
[7] J. Song, M. Alam, A.L. Boehman, U. Kim. (2006). *Combust Flame*. **146**(4):589-604.
[8] M. Salamanca, F. Mondragón, J.R. Agudelo, P. Benjumea, A. Santamaría. (2012). *Combust Flame*. **159**(3):1100-8.
[9] M. Lapuerta, F.J. Martos, J.M. Herreros. (2007). *J Aerosol Sci*. **38**(4):455-66.
[10] R.H. Hurt, G.P. Crawford, H.S. Shim. (2000). *Symp (Int) Combust*. **28**(2):2539-46.
[11] G.A. Stratakis, A.M. Stamatelos. (2003). *Combust Flame*. **132**(1–2):157-69.
[12] K. Yehliu, R.L. Vander Wal, A.L. Boehman. (2011). *Combust Flame*. **158**(9):1837-51.